

# Spinodal decomposition in homogeneous and isotropic turbulence

Prasad Perlekar<sup>1,2</sup>, Roberto Benzi<sup>3</sup>, Herman J.H. Clercx<sup>1</sup>, David R. Nelson<sup>4</sup>, and Federico Toschi<sup>1,5</sup>

<sup>1</sup> Department of Physics and Department of Mathematics and Computer Science and J.M. Burgerscentrum, Eindhoven University of Technology, 5600 MB Eindhoven, The Netherlands; and International Collaboration for Turbulence Research

<sup>2</sup> TIFR Centre for Interdisciplinary Sciences, 21 Brundavan Colony, Narsingi, Hyderabad 500075, India

<sup>3</sup> Dip. di Fisica and INFN, Università “Tor Vergata”, Via della Ricerca Scientifica 1, I-00133 Roma, Italy

<sup>4</sup> Lyman Laboratory of Physics, Harvard University, Cambridge, MA 02138, USA and

<sup>5</sup> CNR, Istituto per le Applicazioni del Calcolo, Via dei Taurini 19, 00185 Rome, Italy

We study the competition between domain coarsening in a symmetric binary mixtures below the critical temperature and turbulent fluctuations. We find that the coarsening process is arrested in presence of turbulence. The physics of the process shares remarkable similarities with the behaviour of diluted turbulent emulsions and the arrest length scale can be estimated with an argument similar to the one proposed by Kolmogorov and Hinze for the maximal stability diameter of droplets in turbulence. Although in the absence of flow the microscopic diffusion constant is negative, turbulence does effectively arrest the inverse cascade of concentration fluctuations by making the low wavelength diffusion constant positive for scales above the Hinze length.

Turbulence is known to strongly increase mixing efficiency. A scalar concentration field in a turbulent flow undergoes a cascade of stretching and folding processes that transfers concentration gradients from large- to small-scales, resulting in efficient mixing on timescales much shorter than those associated with diffusion. The enhanced mixing properties of turbulence arises due its multi-time and multi-scale correlated velocity fluctuations and can be understood in terms of a phenomenological, and scale-dependent, eddy-viscosity  $\nu_t(\ell) \sim \nu(\ell/\eta)^{4/3}$  ( $\eta$  is the Kolmogorov dissipative scale at which velocity fluctuations are dissipated [1]). At larger inertial length scales,  $\ell > \eta$ , the effective diffusivity  $\nu_t \gg \nu$  where  $\nu$  is the kinematic viscosity of the quiescent fluid.

It is well known that a binary liquid mixture cooled below its critical temperature undergoes a phase transition and the mixture separates into phases enriched with its two components. This phenomenon is known as spinodal decomposition. Theoretically, the temperature below which the system undergoes the phase transition is determined by the point where the free-energy minima corresponding to the two phases degenerates [2]. The dynamics of the phase separation can be understood in terms of incompressible Navier-Stokes equations coupled to a Cahn-Hilliard or model-B equations describing the binary mixture order parameter (in the absence of turbulence) [3, 4]. Using dimensional estimates, the evolution of the phase separation can be divided into three regimes: (a) In the initial state, the coarsening length scale of the phase separating binary mixture grows as  $t^{1/3}$  (*Lifshitz-Slyozov scaling*, [5]). This corresponds to growth dominated by the binary mixture diffusivity and is associated with the evaporation of small droplets at the expense of larger growing ones. (b) At intermediate times, when

fluid motion becomes important, and viscous dissipation of the fluid balances the pressure ( $\nu \nabla^2 \mathbf{u} \sim \nabla p$ ) which leads to a linear increase  $\sim t$  in the coarsening length (*Viscous scaling*, [6]). (c) At final stages, the coarsening length scale grows as  $t^{2/3}$  and is governed by the balance of fluid advection with the variations in chemical potential ( $\rho \mathbf{u} \cdot \nabla \mathbf{u} \sim \nabla \mu$ ) (*Inertial scaling*, [7]). This evolution of the coarsening process has been verified in earlier numerical [8–11] and experimental studies [12].

In this letter we study the competition between incompressible turbulence and the coarsening, which leads to a dynamically-active statistically steady state [13]. Turbulence twists, folds, and breaks interfaces into smaller domains whereas coarsening leads to domain growth. We show here that turbulence leads to an arrest of the coarsening length (see Fig. 1). We present state-of-the-art high-resolution numerical simulations of a symmetric liquid binary mixture in three-dimensions in presence of external turbulent forcing. We first verify the presence of the viscous scaling regime in the dynamical coarsening in the absence of turbulence, also observed in earlier simulations of binary mixtures [10, 11]. Next we add an external forcing at large scales to generate homogeneous and isotropic turbulence. Our simulations show that the competition between breakup due to turbulence and coagulation due to spinodal decomposition leads to coarsening arrest. Our results are quantified by observing both the evolution of the concentration power spectrum and the coarsening length scale. We show that the coarsening length-scale can be estimated in terms of the Hinze criterion for droplet breakup [14, 15] pointing at a common physics behind the processes. Finally, we show that the back-reaction of the binary mixture dynamics on the fluid leads to an alteration of the energy cascade.

Early experiments [16, 17] used light scattering to in-

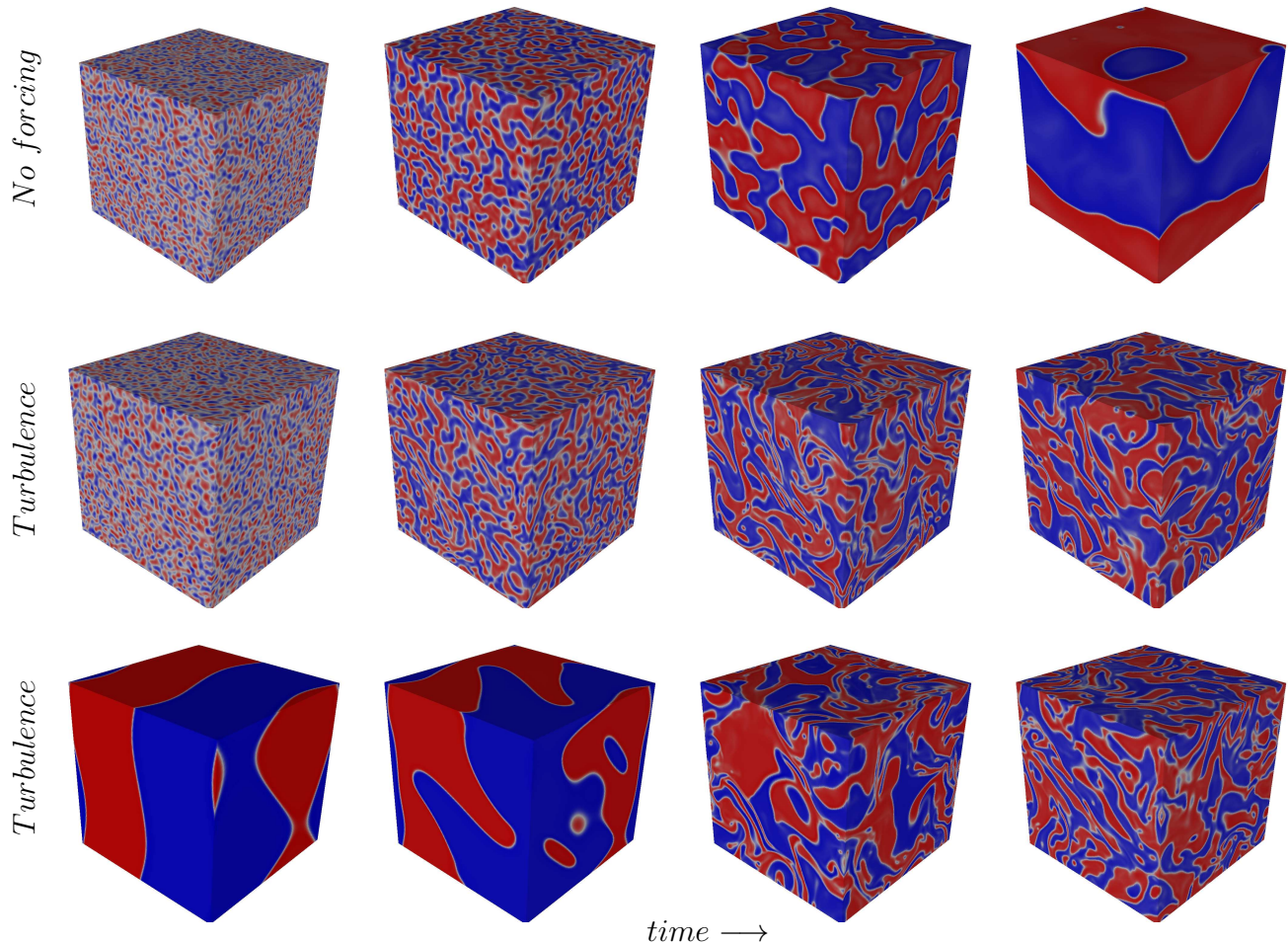


FIG. 1. Pseudocolor plots of the concentration fields, with the two symmetric fluids indicated in red and blue. (Top panel, left-right) Time evolution of the concentration field undergoing coarsening process from a initially well-mixed state. Notice the formation of ever-larger concentration patches as the time evolves. (Middle panel, left-right) Time evolution of the concentration field undergoing coarsening process from a well-mixed state in presence of turbulence generated by external driving. The last two panels indicate that a statistically steady state has developed. The coarsening process goes on uninhibited until arrested by the turbulence at later times. (Bottom panel, left-right) Time evolution of a very coarse phase-separated mixture in presence of turbulence with same intensity as the middle-panel. In this case, the domains are broken up until the mixture attains a steady state domain size that is the same as the one in the middle-panel. This behavior indicates a positive renormalized eddy diffusivity at large length scales even though the microscopic diffusion constant is negative. The Taylor-microscale Reynolds number for the middle and bottom-panel is  $Re_\lambda = 103$  (run ST2, Table I). From the plots it is clear that in case of turbulence the coarsening of concentration gets arrested whereas coarsening length attains domain size in absence of turbulence. In all the panels, the snapshots are taken at times  $t = 5.0 \cdot 10^3, 1.0 \cdot 10^4, 2.5 \cdot 10^4$ , and  $1.0 \cdot 10^5$ .

investigate the coarsening arrest in high-Schmidt number ( $Sc \equiv \nu/D$ ) mixtures where  $D$  is the diffusivity of the binary mixture [18]. These experiments showed that in contrast to the standard coarsening, where a strong light scattering is observed, turbulent stirring induced coarsening arrest exhibits very weak light scattering. These results were later understood by invoking the idea of scale-dependent eddy diffusivity in Ref.[19]. There it was argued that the coarsening would proceed inside the viscous-convective range [20] where the fluid viscosity is important but the diffusivity of the binary mixture can

be ignored. More recent numerical simulations in two-dimensions have studied the effect of chaotic or random velocity fields on the Cahn-Hilliard equation and found that the coarsening is indeed arrested [21–23]. Here, the coarsening length is determined by the balance of the advection of the binary-mixture concentration with gradients in the chemical potential. In Ref. [24] were reported numerical simulations of fully coupled Navier-Stokes and Cahn-Hilliard equations (at  $Sc = 0.1$ ) with externally forced turbulence in two-dimensions in the inverse cascade regime. It was shown that the coarsening length

varies as  $u_{rms}^{-0.41}$ , where  $u_{rms}$  is the root-mean-square velocity.

In this letter, we study coarsening arrest in three-dimensions using state of the art numerical simulations.

To simulate binary mixtures we use a two-component Lattice-Boltzmann method [25–27]. The interaction between the components are introduced using Shan-Chen algorithm [28–30]. The Shan-Chen force, that employs density dependent interactions, is used to introduce non-ideal nature of the fluid [29]. Turbulence is generated by using a large-scale sinusoidal forcing along the three directions. All wave-modes whose magnitude is less than  $\sqrt{2}$  are active and the phases are chosen to be independent Ornstein-Uhlenbeck processes [15].

For all our simulations we used initial conditions with densities  $\rho^{(1)}$  and  $\rho^{(2)}$  such that the corresponding initial order parameter field  $\phi \equiv (\rho^{(2)} - \rho^{(1)})/(\rho^{(2)} + \rho^{(1)})$  is a random distribution of +1 and -1. For simulations with turbulence the forcing was also switched on at the initial time. We simulate in a cubic domain with periodic boundary conditions on all the sides. Table I lists the parameters used in our simulations.

Runs	Domain size	$\rho$	$Re_\lambda$
S1	$128^3$	2.4	NA
S2	$256^3$	2.4	NA
S3	$256^3$	1.1	NA
ST1	$128^3$	2.4	35, 49
ST2	$256^3$	2.4	72, 103
ST3	$512^3$	2.4	103, 162, 185
ST4	$256^3$	1.1	86
NS1	$256^3$	2.4	103
NS2	$512^3$	2.4	162

TABLE I. The parameters of our simulations. Runs S1-3 explore spinodal decomposition in absence of an external forcing, while ST1-ST4 simulate spinodal decomposition in presence of external driving that generates turbulence. For comparing turbulent binary mixture with the standard, single-component turbulent fluid (i.e. symmetric binary mixture above its critical point, without surface tension), we conducted also runs NS1 and NS2. For all the runs, the kinematic viscosity  $\nu = 5 \cdot 10^{-3}$ . For runs S1-3, ST1-3, surface tension  $\sigma = 1.6 \cdot 10^{-3}$ , and the Schmidt number  $Sc = 1.47$  whereas, for the run ST4,  $\sigma = 1.7 \cdot 10^{-3}$ , and  $Sc = 3.72$ . The Taylor scale Reynolds number is  $Re_\lambda \equiv \sqrt{10E}/(\sqrt{\Omega}\nu)$ .

We first investigate how the coarsening proceeds in absence of turbulence in the viscous scaling regime (runs S1-3). As a definition of the coarsening length scale  $L(t)$  we use  $L(t) = 2\pi/[k_1(t)]$ , with  $k_1(t) = (\sum_k k S_k)/(\sum_k S_k)$ , and  $S_k = (\sum_k |\phi_k|^2)/(\sum_k 1)$ . Here  $\phi_k$  is the Fourier transform of  $\phi$ ,  $S_k$  is the shell-averaged concentration spectrum normalized by the corresponding density of states. For the sake of brevity we will call  $S_k$  the concentration spectrum. Finally,  $k = \sqrt{\mathbf{k} \cdot \mathbf{k}}$ , and  $\sum'$  indicates

the summation over all the modes  $k \in [k - 1/2, k + 1/2]$ . Below the critical point, phase separation leads to an  $L(t)$  that grows with time.

For our runs S1-3, as expected [6], we observe  $L(t) \sim t$  [Fig. 2(red dots)].

We now study the effect of turbulence on coarsening. We force large length scales to generate homogeneous, isotropic turbulence in the velocity field. In what follows, we study the effect of turbulence in the viscous scaling regime. Note that  $Sc = \nu/|D| \sim \mathcal{O}(1)$  in our simulations, whereas for most liquid binary mixtures  $Sc \gg 1$ , which requires the resolution of both inertial and the viscous-convective scales to be much higher than what is attained in the present investigation.

Fig. 2 shows how  $L(t)$  increases in the presence of turbulence. Instead of coarsening until  $L(t)$  reaches the size of the simulation domain, turbulence arrests the inverse cascade of concentration fluctuations, blocks coarsening, and leads to a steady state length where the domains constantly undergo coalescence and breakup. The saturating coarsening length  $L_\infty$  decreases with increasing turbulence intensity.

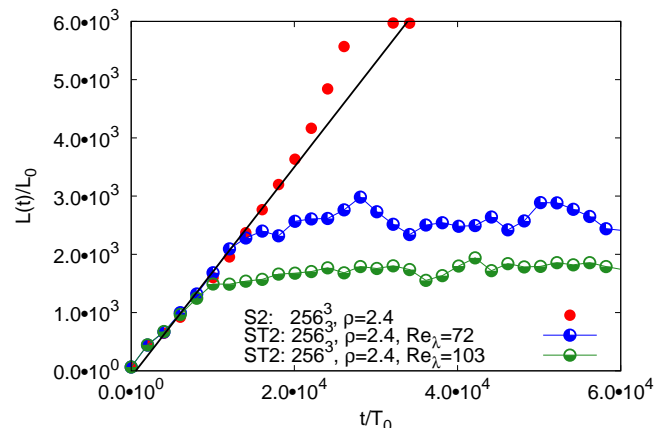


FIG. 2. Coarsening arrest for phase separating binary mixtures in presence of turbulence. In absence of an external turbulent forcing (red circles) the coarsening length keeps on growing as  $L(t) \sim t$  (black line). Switching on turbulence, the coarsening length initially grows undisturbed but then it arrests as the system attains a steady state. Note that for fixed  $\rho$  and surface tension  $\sigma$ , the saturating coarsening length  $L_\infty$  decreases at increasing  $Re_\lambda$ . The time and length scale are non-dimensionalized by the corresponding characteristic length  $L_0 = \nu^2/(\rho\sigma)$  and time  $T_0 = \nu^3/(\rho\sigma^2)$ .

In an earlier study [15], we had shown that for asymmetric binary mixtures the Hinze criterion provides an estimate for the average droplet diameter undergoing breakup and coalescence in turbulence. We now show that even for 50% – 50% binary mixtures, the Hinze criterion gives a good estimate for the coarsening length scale  $L_\infty$  at long times.

According to the prediction of Ref. [14], the maximum

droplet diameter that can be stable to turbulent velocity fluctuations in the steady state should be given by the Hinze length

$$L_H \approx \left(\frac{\rho}{\sigma}\right)^{-3/5} \epsilon^{-2/5}. \quad (1)$$

Actually the above equation is also consistent with the predictions of Ref. [31]. A general criteria for the coarsening length is given by the relation  $L(t) = L_0 f(x)$  with  $x = t/T_0$  [31]. The function  $f(x)$  satisfies the two limiting scaling  $f(x) \sim x$  for small  $x$  and  $f(x) \sim x^{2/3}$  for large  $x$ . In turbulent flow, the relevant time scale is given by  $L/\delta v(L)$  where  $\delta v(L)$  is the size of the velocity fluctuation at the scale  $L$ . Since this time scale is much longer than  $t$ , the appropriate scaling behavior for  $f(x)$  is  $x^{2/3}$ . Using the inertial scaling we again obtain Eq. (1). The above argument may not apply to shear flows, due to non isotropic contributions and strong dissipation at the boundaries, and in two dimensional flows where the characteristic time scale is dictated by enstrophy cascade.

In [15, 32] it was shown that in presence of coagulation-breakup processes the correct quantity to look at is the average droplet diameter  $L_\infty \equiv \langle L(t) \rangle$  in the statistically stationary state. Therefore we expect that the ratio  $L(t)/L_H$  stay constant in all our simulations. The plot in Fig. 3 shows the plot of  $L(t)/L_H$  for our runs.

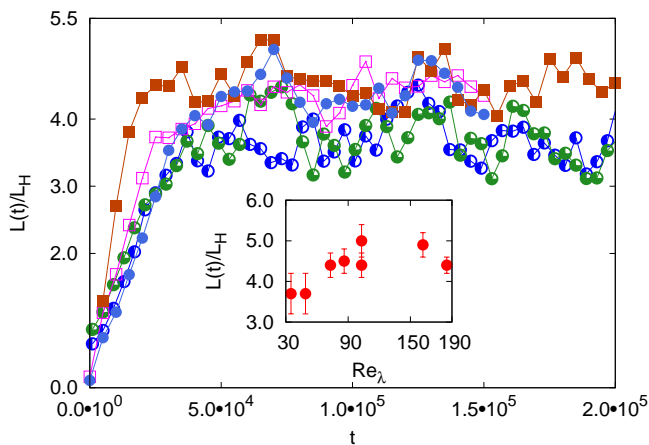


FIG. 3. Growth of the coarsening length scale  $L(t)$  in the arrested state normalized by the Hinze length  $L_H$  for  $Re_\lambda = 35, 49$  (blue three-quarter-filled circle and green half-filled circle) [run ST1],  $Re_\lambda = 72, 103$  (purple square and brown filled square) [run ST2], and  $Re_\lambda = 86$  (blue filled circle) [run ST4]. In the inset we plot the average value of  $L(t)/L_H$ , calculated over the time window  $t = 5 \times 10^4$  to  $2 \times 10^5$ , for different Reynolds numbers  $Re_\lambda$ . Within error bars,  $L(t)/L_H \approx 4.4 \pm 0.5$  is found to be a good indicator for the arrested length scale. We believe that the smaller value of  $L(t)/L_H$  (although within our error bars) for the  $Re_\lambda = 35, 49$  arises because of the lower grid resolution. .

The blockage of the energy transfer by turbulence is best understood in Fourier space. The plots in Fig-

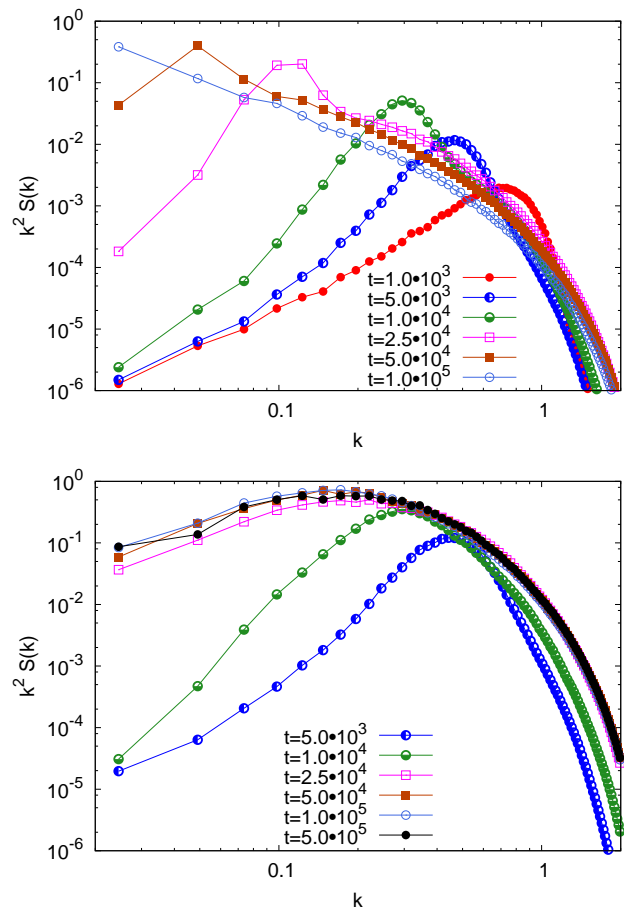


FIG. 4. (Top panel) The inverse cascade of concentration spectrum  $k^2 S(k)$  for spinodal decomposition at times  $t = 10^3 - 5 \cdot 10^5$  ( $256^3, \rho = 2.4$  [run S2]) without turbulence. The Fourier mode associated with the peak of the spectrum gives an estimate of the instantaneous coarsening length. The peak shifts towards the small wave vectors (large length scales) as time progresses. On the other hand, in presence of turbulence (bottom panel,  $\{256^3, \rho = 2.4, \text{ and } Re_\lambda = 103$  [run ST2]}), we do observe an initial inverse cascade of concentration that saturates around  $t = 5 \cdot 10^4$  indicating a blockage of the inverse cascade.

ure 4 compare the concentration spectrum  $k^2 S_k$  at various times  $t = 10^3, 10^4, \text{ and } 10^5$  in absence ( $256^3, \rho = 2.4$  [run S2]) and presence ( $256^3, \rho = 2.4, \text{ and } Re_\lambda = 103$  [run ST2]) of turbulence. Without turbulence we observe a peak in the concentration spectrum at initial times that moves towards smaller wave vectors until it reaches the domain size. On the other hand in presence of turbulence, the concentration fluctuations saturate and the concentration spectrum reaches a steady state.

The presence of a surface tension should also alter the transfer of energy in Fourier space. The stretching and folding of the surface by turbulence takes energy from the fluid. On the other hand in the regions of weak turbulence local chemical potential will transfer energy back to the fluid. In Fig. 5 we investigate how a phase separating

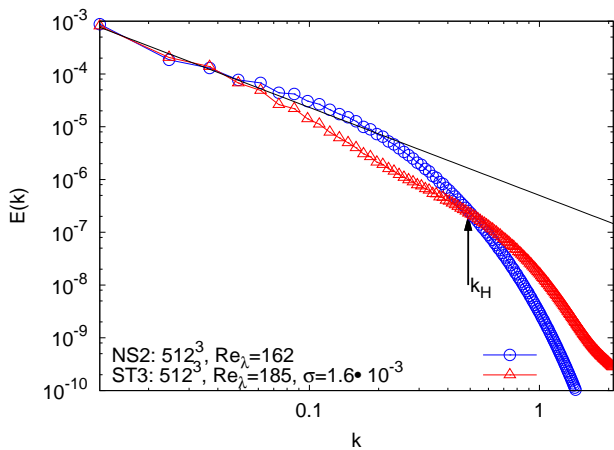


FIG. 5. Comparison of the energy spectrum for the spinodal decomposition in presence of turbulence (triangle, run ST3 [ $Re_\lambda = 185$ ]) with the pure fluid case (circle, run NS2). The black line indicates the Kolmogorov scaling  $k^{-5/3}$ . We observe that the energy content of the binary mixture is lower than the pure fluid case in the inertial range but in the deep-dissipation range it is higher. We find that the large- $k$  cross-over takes place roughly around the inverse Hinze scale  $k_H \equiv 1/L_H$ . This cross-over was also confirmed by comparing runs NS1 and ST2 (not shown here).

binary liquid mixture velocity spectrum compares with the pure fluid case. We observe that in the inertial range the energy content of the binary mixture is strongly suppressed in comparison to the pure fluid case whereas, in the dissipation range the energy content is higher for the binary mixture. Qualitatively this phenomenon is similar to the case of dilute polymer solutions in turbulence where the polymer elasticity is shown to alter the energy transfer in a similar way [33, 34]. However, we note that the main difference between polymers and binary mixture interface dynamics is that the size of polymers is smaller than the dissipation range whereas, in the present study, the droplet size lie in the inertial range of scales.

We acknowledge the COST Action MP0806 and FOM (Stichting voor Fundamenteel Onderzoek der Materie) for support. We acknowledge computational support from CASPUR (Roma, Italy), from CINECA (Bologna, Italy), and from JSC (Juelich, Germany). This research was supported in part by the National Science Foundation under Grant No. PHY11-25915. Work by DRN was supported by the National Science Foundation (USA) via Grant DMR 1005289 and through the Harvard Materials Research Science and Engineering Laboratory, through Grant DMR 0820484.

- [1] W. Richardson, Proc. R. Soc. London, Ser. A **110**, 709 (1926).
- [2] K. Dill and S. Bromberg, *Molecular Driving Forces* (Garland Science, New York, 2003).
- [3] J. Cahn, Trans. Metall. Soc. AIME **242**, 166 (1968).
- [4] P. Hohenberg and B. Halperin, Rev. Mod. Phys. **49**, 435 (1977).
- [5] I. Lifshitz and V. Slyozov, J. Phys. Chem. Solids **19**, 35 (1959).
- [6] E. D. Siggia, Phys. Rev. A **20**, 595 (1979).
- [7] H. Furukawa, Phys. Rev. A **31**, 1103 (1985).
- [8] T. Lookman, Y. Wu, F.J. Alexander, and S. Chen, Phys. Rev. E **53**, 5513 (1996).
- [9] V.M. Kendon, Phys. Rev. E **61**, 6071 (2000).
- [10] I. Pagonabarraga, J.-C. Desplat, A. J. Wagner, and M. E. Cates, New J. Phys. **3**, 9 (2001).
- [11] N. Gonzalez-Segredo, M. Nekovee, and P.V. Coveney, Phys. Rev. E **67**, 046304 (2003).
- [12] J. Hobley, S. Kajimoto, A. Takamizawa, and H. Fukumura, Phys. Rev. E **73**, 011502 (2006).
- [13] R. Ruiz and D. R. Nelson, Phys. Rev. A **23**, 3224 (1981).
- [14] J. Hinze, A.I.Ch.E. Journal **1**, 289 (1955).
- [15] P. Perlekar et al., Phys. Fluids **24**, 065101 (2012).
- [16] D. J. Pine, N. Easwar, J. V. Maher, and W. I. Goldburg, Phys. Rev. A **29**, 308 (1984).
- [17] P. Tong, W. I. Goldburg, J. Stavans, and A. Onuki, Phys. Rev. Lett. **62**, 2668 (1989).
- [18] Ref. [19] use Prandtl number instead of Schmidt. To be consistent with the mixing of a scalar in turbulence we use Schmidt number.
- [19] J.A. Aronovitz and D. R. Nelson, Phys. Rev. A **29**, 2012 (1984).
- [20] G. Batchelor, J. Fluid Mech. **5**, 113 (1959).
- [21] A. M. Lacasta, J. M. Sancho, and F. Sagues, Phys. Rev. Lett. **75**, 1791 (1995).
- [22] L. Berthier, J.L. Barrat, and J. Kurchan, Phys. Rev. Lett. **86**, 2014 (2001).
- [23] L.ÓNáirigh, and J.L. Thiffeault, Phys. Rev. E **75**, 016216 (2007).
- [24] S. Berti, G. Boffetta, M. Cencini, and A. Vulpiani, Phys. Rev. Lett. **95**, 224501 (2005).
- [25] U. Frisch et al., Complex Systems **1**, 649 (1987).
- [26] M. Sukop and J. D.T. Throne, *Lattice Boltzmann Modeling: An Introduction for Geoscientists and Engineers* (Springer, Springer Berlin Heidelberg New York, 2007).
- [27] S. Succi, *The Lattice Boltzmann Equation for Fluid Dynamics and Beyond* (Oxford, Oxford University Press, UK, 2001).
- [28] X. Shan and H. Chen, Phys. Rev. E **47**, 1815 (1993).
- [29] X. Shan and H. Chen, Phys. Rev. E **49**, 2941 (1994).
- [30] X. Shan and G. Doolen, J. Stat. Phys. **81**, 379 (1995).
- [31] M. Cates, Lecture Notes for les Houches 2012 Summer School on Soft Interfaces; arXiv:1209.2290 (2012).
- [32] L. Biferale et al., J. Phys: Conf Ser **318**, 052017 (2011).
- [33] P. Perlekar, D. Mitra, and R. Pandit, Phys. Rev. Lett. **97**, 264501 (2006).
- [34] E. D. Angelis, C. Casciola, R. Benzi, and R. Piva, J. Fluid Mech. **531**, 1 (2005).